ORIGINAL PAPER

CrossMark

Amperometric determination of ascorbic acid with a glassy carbon electrode modified with TiO$_2$-gold nanoparticles integrated into carbon nanotubes

Jessica Scremin[1] · Eduardo César Melo Barbosa[2] · Carlos Alberto Rossi Salamanca-Neto[1] · Pedro Henrique Cury Camargo[2] · Elen Romão Sartori[1]

Abstract

A glassy carbon electrode was modified with a TiO$_2$-gold nanoparticle hybrid integrated with multi-walled carbon nanotubes in a dihexadecylphosphate film (TiO$_2$-Au NP-MWCNT-DHP/GCE) and applied to amperometric determination of ascorbic acid (AA). The modified sensor displays fast charge transfer and shows an irreversible anodic behavior for AA by cyclic voltammetry. Under optimal experimental conditions and using amperometry at 0.4 V, the analytical curve presented a statistical linear concentration range for AA from 5.0 to 51 µmol L^{-1}, with a limit of detection of 1.2 µmol L^{-1}. The electrode was successfully applied to the determination of AA in pharmaceutical and fruit juice without the need for major pretreatment of samples.

Keywords Electrochemical sensing · Modified electrode · Nanostructured material · Hybrid material · Pharmaceuticals

Introduction

Ascorbic acid (AA), usually known as vitamin C, is not synthesized by the human body, and should be ingested through diet and vitamin supplements. The food industry employs AA as food additive (E300) to prevent the oxidation, maintaining the taste, texture and appearance of food for a longer time period [1, 2]. In addition, it is commonly used in many chemical, pharmaceutical and clinical procedures, as well as in environmental and industrial processes. Thus, accurate determination of AA is necessary in various sample types. AA is electrooxidized on conventional electrode surfaces, such as

boron-doped diamond electrode [3] and glassy carbon electrode (GCE) [4], but this process occurs with high overpotentials. The use of a chemically modified electrode, mainly with nanostructure materials, tends to improve sensitivity and selectivity in the electrochemical AA determination.

Several studies have demonstrated the use of these types of electrodes for AA determination [5–10]. Fernandes et al. developed a GCE modified with multi-walled carbon nanotubes (MWCNTs) and MnFe$_2$O$_4$ nanoparticles (NPs) (MnFe$_2$O$_4$-MWCNT/GCE) [5]. Kannan and John determined AA in blood serum and urine using an Au NPs self-assembled to 2,5-dimercapto-1,3,4-thiadiazole (DMT) monolayer modified gold electrode (Au NP-DMT/Au) [6]. Hosseini et al. modified a titanium electrode by galvanic deposition of Au NPs on TiO$_2$ nanotube substrates (Au NP-TiO$_2$/Ti) for AA determination in pharmaceutical and clinical samples [7]. Aneesh et al. reported the development of a modified GCE with partially reduced graphene oxide (RGO-GCE) for AA determination in serum samples [8]. Taleb et al. described the fabrication of a GCE modified with graphene onto a network of alumina nanofibers (graphene-ANF-C700/GCE) for simultaneous determination of AA, dopamine (DA) and uric acid (UA) in spiked urine sample [9]. Zhao et al. developed a modified GCE with nanoporous PtCu alloy (PtCu alloy/GCE) for simultaneous determination of AA, DA and UA [10]. All these

✉ Elen Romão Sartori
elensartori@uel.br

[1] Departamento de Química, Centro de Ciências Exatas, Universidade Estadual de Londrina (UEL), Rodovia Celso Garcia Cid, PR 445 Km 380, PR, C.P. 10.011, Londrina 86057-970, Brazil

[2] Departamento de Química Fundamental, Instituto de Química, Universidade de São Paulo, Av. Prof. Lineu Prestes, 748, São Paulo, SP 05508-000, Brazil

authors reported that the modified electrodes remarkably improve the electrocatalytic activity towards the oxidation of AA with an increase in the anodic peak current.

Advances in development of new nanostructured materials have attracted considerable attention in recent years, particularly with respect to modification of electrode surfaces for various purposes and applications. Artificial hybrids represent one of the most growing classes of materials for achieving improved versatility in a variety of applications including sensors, biosensors, drug delivery, catalysis, and energy conversion/storage [11–15]. They have complementary properties and unique characteristics that are not matched by their individual counterparts. This becomes even more pronounced when at least one of the components present nanoscale features [16]. For instance, good electrical conductivity, high surface areas, high uniformity, and high electrocatalytic activities have been reported [17]. These properties enable applications, for example, in the development of electrochemical sensors. In this case, the optimization over the choice and morphological features of the employed materials may lead to better sensitivities, limit of detection (LOD), and selectivities [18–20].

Among the many materials that have been employed for analytical applications, TiO2-Au NPs represents an interesting material for sensor development [21, 22]. For example, Zhou et al. developed a sensitive and selective electrochemical sensor based on the modification of a gold electrode with Au NP-TiO2 for the determination of mercury ions (Hg^{2+}) in water samples [21]. Au NP-TiO2 with average sizes of 5–15 nm was synthesized via a sol-gel method. In another example, Ampelli et al. prepared Au NP-embedded TiO2 composites by wet impregnation of TiO2 with Au NPs. It was deposited on a commercial carbon screen-printed electrode for monitoring glucose in fermentation processes, without ethanol interference [22]. Even though TiO2-Au NP hybrids have been widely reported, most systems are still characterized by a poor control over the size, shape, and relative spatial distribution of TiO2 and Au NPs.

Damato et al. [23] demonstrated a new and environmentally friendly strategy for the synthesis of TiO2-Au NPs hybrid materials comprised of TiO2 colloidal spheres decorated with Au NPs. It displayed monodisperse size and uniform dispersion over the TiO2 surface. This synthesis was based on the utilization of TiO2 colloidal spheres as seeds for Au NPs deposition employing $AuCl_4^-$ as precursor, AA as a reducing agent, polyvinylpyrrolidone (PVP) as stabilizer and water as solvent. This material, when integrated with carbon black in the modification of the GCE, displayed good electrocatalytic performances towards the in situ production of H_2O_2 via the oxygen reduction [24].

In this context, a GCE was modified with TiO2-Au NPs hybrids and functionalized MWCNTs within a film of the surfactant dihexadecylphosphate (DHP) (referred to as TiO2-Au NP-MWCNT-DHP/GCE) for amperometric determination of AA. The method was applied for analysis of commercially available pharmaceutical formulation and fruit juice samples with the results in good accordance with those obtained by reference iodometric titration method [25]. The analytical parameters of the TiO2-Au NP-MWCNT-DHP/GCE as well as its reproducibility, stability and selectivity were also evaluated. The potentiality of its use for simultaneous determination of AA and sulfite, or AA and other compounds of biological interest, such as UA and DA, is also here presented.

Experimental

Reagents and solutions

All chemicals were of analytical grade: AA, DHP, and MWCNTs (20–30 nm in diameter and 0.5–2 μm in length; purity: ≥ 95%) (Sigma-Aldrich, http://www.sigmaaldrich.com) and potassium chloride salt (KCl; Merck, http://www.merck.com.br). All chemicals were used without further purification.

All solutions were prepared with ultra-purified water (resistivity ≥18.2 MΩ cm) supplied by Milli-Q system (Millipore water Ltd., USA, www.millipore.com). The samples containing AA (pharmaceutical and juice fruit) were acquired in a local pharmacy and supermarket, respectively, in Londrina, Brazil.

For the synthesis of the materials, $HAuCl_4 \cdot 3H_2O$ (hydrogen tetrachloroaurate trihydrate, 48% in gold, Sigma-Aldrich, http://www.sigmaaldrich.com), PVP (Sigma-Aldrich, http://www.sigmaaldrich.com, MW 55000 g mol^{-1}), EG (ethylene glycol, 99.5%, Synth), acetone (99.5%, Synth), acetic acid (99.7%, Synth) and Ti(OBu)4 (titanium butoxide, 97%, Sigma-Aldrich, http://www.sigmaaldrich.com) were used as received.

The supporting electrolyte was a 0.10 mol L^{-1} KCl solution. A stock solution of 10 mmol L^{-1} AA was freshly prepared in this supporting electrolyte. Working solution of AA was prepared by the dilution of this stock solution with 0.10 mol L^{-1} KCl solution prior to using. AA solutions were protected from light by using amber glass material.

Apparatus

All voltammetric/amperometric measurements were carried out using a FRAII μAutoLab type III potentiostat/galvanostat (Metrohm Autolab B. V., Netherlands, http://www.ecochemie.nl) controlled by the general purpose electrochemical system (GPES) software. A conventional three-electrode glass cell was employed, using a platinum plate as the auxiliary electrode, Ag/AgCl (3.0 mol L^{-1} KCl) as the reference electrode and TiO2-Au NP-MWCNT-DHP/GCE as the working electrode. GCE was obtained from Tokay Carbon Co., Japan (3 mm, diameter) and carefully polished sequentially with metallographic abrasive paper (# 6) and

slurries of 0.3 and 0.05 μm alumina. Subsequently, it was sonicated for 5 min in acetone and ultrapure water, and dried at room temperature prior to modification.

The electrochemical impedance spectroscopy (EIS) experiments were performed at the formal potential of the $[Fe(CN)_6]^{4-}/[Fe(CN)_6]^{3-}$ redox pair, from 10 mHz to 100 KHz (10 points per decade) and with a 10 mV (rms) ac perturbation, for 5.0 mmol L^{-1} $K_3[Fe(CN)_6]$ in 0.10 mol L^{-1} KCl solution.

The pH of solutions was measured using a pHmeter (Hanna Instruments, USA, https://hannainst.com), model HI-221, employing a combined glassy electrode with an Ag/AgCl (3.0 mol L^{-1} KCl) external reference electrode.

The microscopy images were obtained by a scanning electron microscope (SEM) JOEL FEG-SEM JSM 6330F (JOEL, USA, https://www.jeolusa.com) operated at 5 kV. SEM samples were prepared by drop-casting an aqueous suspension of the particles on a Si wafer and on glassy carbon plate, then, dried under ambient conditions. The particle size distribution was obtained by measuring the diameters of 200 particles from the SEM images.

Synthesis of TiO₂-Au NPs

TiO₂ colloidal spheres and Au NPs spheres were synthesized according to a procedure previously described in the literature [23]. Typically, a mixture containing 1 mL of Ti(OBu)₄ and 22.5 mL of EG was stirred for 8 h at room temperature. Next, it was poured into a mixture containing 100 mL of acetone 1.25 mL of water and 0.4 mL of acetic acid, which was then kept under vigorous stirring at room temperature for 2 h and at rest for 3 more hours. At this point, titanium glycolate microspheres were formed. These samples were washed thoroughly using ethanol and precipitating through centrifugation. The following step consisted of suspending these particles in 50 mL water and keeping it under stirring at 70 °C for 8 h, producing TiO₂ spheres, which were washed with ethanol and water. The final product was suspended in 100 mL of water. In order to decorate the spheres, 6 mL of the TiO₂ suspension were added to a solution containing 12 mL of water, 120 mg of ascorbic acid and 70 mg of PVP. This orange mixture was kept under stirring for 10 min at 90 °C and at this point, 6 mL of a 1.0 mmol L^{-1} $AuCl_4^{1-}$ solution were quickly added to the mixture, producing a red suspension. This reaction was stopped after 30 min, producing TiO₂-Au NPs.

Preparation of working electrode

Prior to preparing the dispersion, MWCNTs were purified with 2.0 mol L^{-1} HCl solution followed by its functionalization with an acid treatment, using a mixture of nitric and sulfuric acid (HNO₃:H₂SO₄, 3:1, v/v), as described in the literature [26].

The TiO₂-Au NP-MWCNT-DHP film was prepared by sonicating 1.0 mg of the functionalized MWCNTs and 1.0 mg DHP in 1 mL of ultrapure water for 30 min, as described by Ardila et al. [27]. Then, 25 μL of a solution of TiO₂-Au NPs hybrid material were added to 50 μL of the MWCNfT/DHP suspension. 10 μL of the final mixture was dropped onto the surface of a GCE. The solvent was dried at room temperature after 2 h, and a homogenous and uniform TiO₂-Au NP-MWCNT-DHP film was formed on the GCE surface. The modified GCE was then placed in the electrochemical cell containing 0.10 mol L^{-1} KCl solution and ten cycles were applied in a potential window from −0.20 to 0.70 V at a scan rate 100 mV s^{-1} using a cyclic voltammetry (CV) method to obtain stable responses.

General analytical procedures

CV was used for the electrochemical characterization of the modified electrode and for the voltammetric behavior of AA. Amperometry was used to quantify AA in pharmaceutical and food samples.

After optimizing the experimental parameters for the method, an analytical curve was constructed by adding small volumes of a standard AA solution in the electrochemical cell containing 10 mL of 0.10 mol L^{-1} KCl solution. The LOD value was calculated using the formula $3S/M$, where S is the standard deviation of ten measurements of the blank solution and M is the slope of the analytical curve. The statistical parameters were obtained using the IBM SPSS Statistics software with significance level of 5%.

To prepare the pharmaceutical sample, ten tablets (500 mg AA per tablet) were accurately weighed (average weight of 588.1 ± 19 mg) and powdered in a mortar. An accurately amount of relative of one tablet was transferred into a 50 mL volumetric flask containing the supporting electrolyte (0.10 mol L^{-1} KCl solution). Afterward, 5.0 μL of this solution was transferred to the electrochemical cell containing 10 mL of 0.10 mol L^{-1} KCl solution and the amperograms were obtained.

To prepare the juice sample, 3 mL of the orange juice were pipetted into a 50 mL volumetric flask containing the supporting electrode (0.10 mol L^{-1} KCl solution). Then, 200 μL were transferred to the electrochemical cell containing 10 mL of 0.10 mol L^{-1} KCl solution and the amperograms were obtained.

The AA concentration in each sample was determined by using the analytical curve previously obtained in the optimum experimental conditions. The measurements were done in triplicate for each sample to ensure significance in the results.

The iodometric titration method was used as reference for AA determination in the food and pharmaceutical samples [25]. For this purpose, a 50.0 mmol L^{-1} iodide solution was

employed as titrant; and starch was used as indicator for adequate visualization of the titration endpoint.

Results and discussion

Morphological characterization of the TiO₂-Au NPs

The size and morphology of the TiO₂-Au NPs was characterized by SEM. The SEM images for TiO₂ colloidal spheres and the TiO₂-Au NPs hybrids are presented in Fig. 1a and b, respectively. The TiO₂ colloidal spheres displayed spherical shapes and monodisperse sizes, being 267.8 ± 37.8 nm, in diameter (Fig. 1a). It can be observed that there was no modification of the TiO₂ size and shape after the deposition of Au NPs (Fig. 1b). Moreover, the deposited Au NPs are homogeneously distributed over the TiO₂ surface without significant aggregation. The deposited Au NPs presented an average diameter of 9.7 ± 2.2 nm over the TiO₂ surface. In this hybrid material, it is expected that there will be interactions between Au NPs (metal) and TiO₂ (semiconductor) that favors the occurrence of reactive sites and electron transfer processes [28].

Fig. 2 shows the SEM images obtained for different modifications of GCE surface. A clear difference in terms of surface roughness was observed among these electrodes. It can
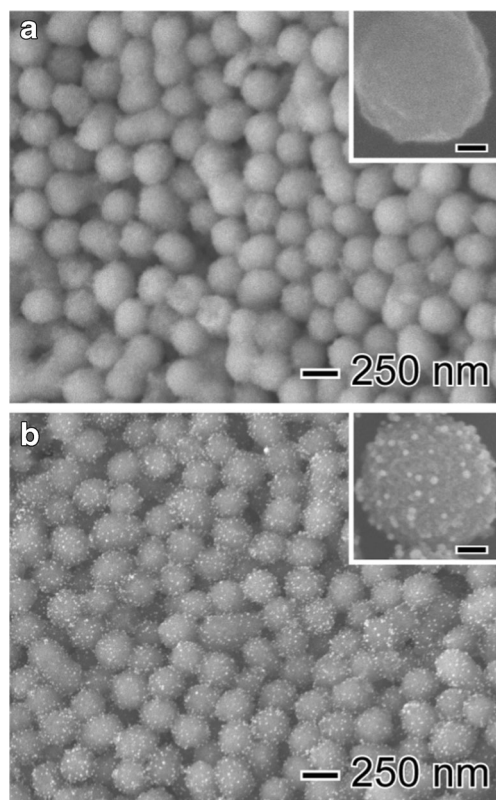

Fig. 1 SEM images obtained for the (**a**) TiO₂ colloidal spheres and (**b**) TiO₂-Au NPs hybrids. All inset bars correspond to 50 nm

be seen in Fig. 2c that a relatively dense film was formed and the GCE surface was completely covered with functionalized MWCNTs, when compared to unmodified GCE (Fig. 2a). On Fig. 2d, the TiO₂-Au NPs hybrid material was homogeneously distributed on the MWCNTs, and presented uniform sizes relative to TiO₂-Au NP-DHP/GCE (Fig. 2b).

Electrochemical characterization

The GCE and modified electrodes were characterized by CV and EIS techniques in the presence of $K_3[Fe(CN)_6]$ as electroactive species. The results from all electrodes were compared in order to evaluate the advantages of using TiO₂-Au NPs hybrids integrated with the MWCNTs. The integration of functionalized MWCNTs and the TiO₂-Au NPs hybrid enables a better distribution of TiO₂-Au NPs in the film with high electroactive area, as will be shown below. The measurements were performed for a 0.10 mol L^{-1} KCl solution containing 5.0 mmol L^{-1} $K_3[Fe(CN)_6]$.

Cyclic voltammograms of GCE and modified electrodes for $K_3[Fe(CN)_6]$ are shown in Fig. 3a. As can be clearly observed, the response to hexacyanoferrate(III) is decreased by the DHP coating (DHP/GCE or TiO₂-Au NP-DHP/GCE) when compared with the unmodified electrode (GCE), meaning that this surfactant is causing a small decrease in the electroactive surface of the electrode due to its poor conductivity. This partially blocking of the electrode was previously reported in the literature [29]. On the other hand, when MWCNTs were added to the film coating, an increase in the response occurred. This effect is further enhanced by the addition of the hybrid material (TiO₂-Au NP-MWCNT-DHP/GCE). The coupling of TiO₂-Au NP-MWCNTs produces an improvement in the electron transfer between hexacyanoferrate(III) and the GCE surface, since they combine the excellent properties of MWCNTs and TiO₂-Au NPs [26, 30]. The same figure also shows differences among the process reversibility of $K_3[Fe(CN)_6]$ using different sensors. The difference between cathodic and anodic peaks (ΔE) are 103.5, 310.5, 235.2, 85.4 and 81.6 mV for GCE, DHP/GCE, TiO₂-Au NP-DHP/GCE, MWCNT-DHP/GCE and TiO₂-Au NP-MWCNT-DHP/GCE, respectively. The lower ΔE value presented by TiO₂-Au NP-MWCNTs-DHP/GCE indicate that its electron transfer is faster when compared with other sensors. [31] In all cases, at the bare GCE or modified electrode, curves of I vs $v^{1/2}$ for the oxidation process (data not shown) were obtained, consistent with a diffusion-controlled process [31]. By applying the Randles-Sevick equation and using a diffusion coefficient for $K_3[Fe(CN)_6]$ of 7.6×10^{-6} cm^2 s^{-1} [32], the electroactive area for GCE, DHP/GCE, TiO₂-Au NP-DHP/GCE, MWCNT-DHP/GCE and TiO₂-Au NP-MWCNT-DHP/GCE was estimated as 0.0423, 0.0078, 0.0208, 0.0439, and 0.0606 cm^2, respectively. The results above suggest that hybrid material integrated with carbon nanotube modification yielded a higher electroactive area.

Fig. 2 SEM images of (**a**) GCE surface, (**b**) TiO$_2$-Au NP-DHP/GCE, (**c**) MWCNT-DHP/GCE and (**d**) TiO$_2$-Au NP-MWCNT-DHP/GCE
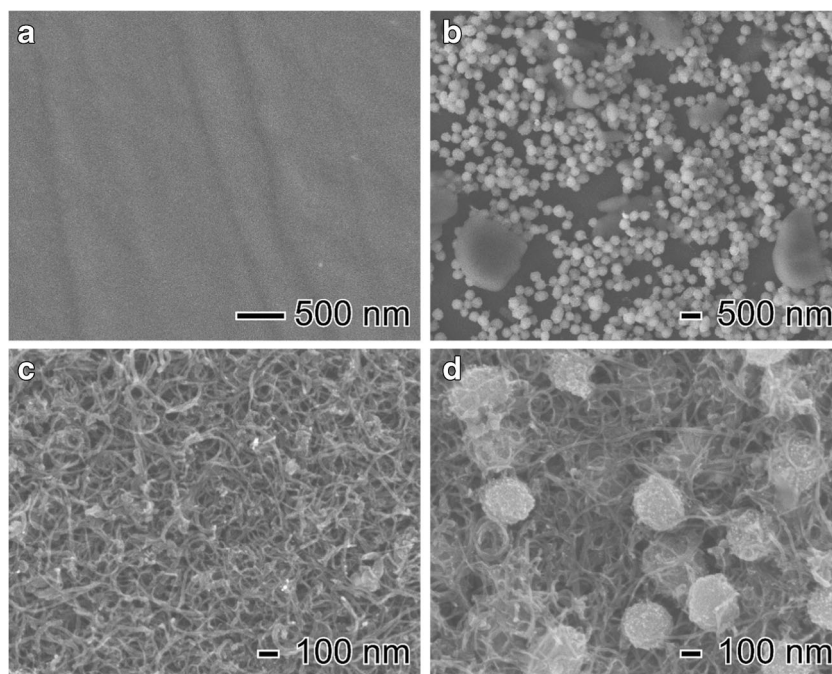
EIS analysis was performed to provide information about interfacial properties of the surface of the GCE caused by the presence of different modifiers. The Nyquist plots obtained for GCE, DHP/GCE, TiO$_2$-Au NP-DHP/GCE, MWCNTs-DHP/GCE and TiO$_2$-Au NP-MWCNTs-DHP/GCE in the presence of K$_3$[Fe(CN)$_6$] are shown in Fig. 3b. In these plots, the diameter of semicircular portion at higher frequencies is directly related to the electron transfer resistance (R$_{et}$), and a linear portion at lower frequencies, representing the diffusion processes. Table S1 (Supplementary materials) shows the values of charge-transfer resistance of each electrode. It can be observed that the DHP/GCE and TiO$_2$-Au NP-DHP/GCE displayed a larger semicircle, indicating that there is an increase in the electron transfer resistance. Despite the high conductivity of the hybrid material, DHP has poor conductivity, introducing a resistance into the electrode-solution and/or a decrease in the diffusion of K$_3$[Fe(CN)$_6$] through of films. One can also observe a decrease of the semicircle diameter for the modified GCE with nanotubes or TiO$_2$-gold NPs integrated with nanotubes, indicating an improvement of the electron transfer rate on the electrode surface compared to the unmodified GCE. In addition, the apparent standard heterogeneous rate constant (k'_0) for each electrode was calculated according to Eq. 1 [33]:

$$k'_0 = \frac{RT}{n^2 F^2 R_{et} AC} \tag{1}$$

where R is the gas universal constant, T is the thermodynamic temperature (298.15 K), F is the Faraday's constant (96,485 C mol^{-1}), A is the geometric area in cm^2 and C is the concentration of the K$_3$[Fe(CN)$_6$] at the supporting electrolyte solution in mol cm^{-3}. By comparing our results with those presented in the Table S1 (Supplementary materials), it is clear that with TiO$_2$-Au NPs-MWCNTs-DHP/GCE the k'_0 value is larger than other electrodes, indicating faster electron-transfer. These results demonstrate the contribution of the hybrid material and carbon nanotubes for the improvement of the GCE electrochemical performance and are in concordance with those obtained from ΔE values.

Study of electrochemical behavior of ascorbic acid on the modified electrodes

Although addition of hybrid material into MWCNTs-DHP/GCE gave little influence to redox current of K$_3$[Fe(CN)$_6$], the addition gave significant influence to that of AA, thus, this analyte was used to demonstrate the potential of this new platform for analytical purposes.

The electrochemical behavior of the AA molecule was investigated by CV in the potential range of −0.20 to 0.70 V. In Fig. 4, the cyclic voltammograms were obtained using GCE, DHP/GCE, TiO$_2$-Au NP-DHP/GCE, MWCNT-DHP/GCE and TiO$_2$-Au NP-MWCNT-DHP/GCE in a 0.10 mol L^{-1} KCl solution in the presence of 0.10 mmol L^{-1} AA. In all cases, an oxidation process was observed during the anodic potential scanning, with the absence of a reduction process during the cathodic one. This suggests that AA underwent an irreversible oxidation reaction. From the results shown in Fig. 4, the AA voltammetric response on all electrodes were evaluated and verified that the TiO$_2$-Au NP-MWCNT-DHP/GCE presented the higher anodic peak current and smaller potential than that obtained on unmodified GCE. These
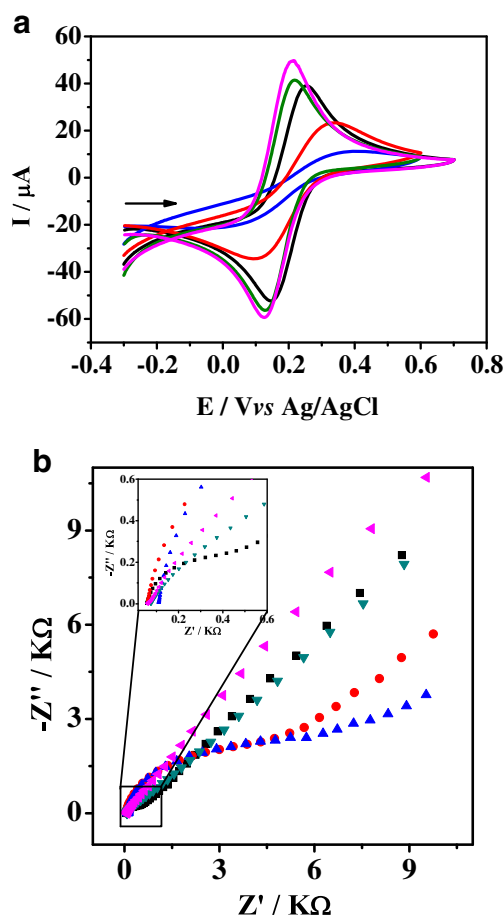
Fig. 4 Cyclic voltammograms recorded at 50 mV s^{-1} for 0.10 mmol L^{-1} AA prepared in 0.10 mol L^{-1} KCl with working electrodes: (——) GCE, (——) DHP/GCE, (——) TiO$_2$-Au NPs-DHP/GCE, (——) MWCNTs-DHP/GCE and (——) TiO$_2$-Au NPs-MWCNTs-DHP/GCE

Fig. 3 Analytical characterization of the electrodes: (a) cyclic voltammograms (50 mV s^{-1}), after background subtraction, of 5.0 mmol L^{-1} K$_3$[Fe(CN)$_6$] in a 0.10 mol L^{-1} KCl solution at (——) GCE, (——) DHP/GCE, (——) TiO$_2$-Au NPs-DHP/GCE, (——) MWCNTs-DHP/GCE and (——) TiO$_2$-Au NPs-MWCNTs-DHP/GCE. (b) EIS diagrams obtained for 5.0 mmol L^{-1} K$_3$[Fe(CN)$_6$] in 0.10 mol L^{-1} KCl solution using (■) GCE, (▲) DHP/GCE, (●) TiO$_2$-Au NPs-DHP/GCE, (▼) MWCNTs-DHP/GCE and (◄) TiO$_2$-Au NPs-MWCNTs-DHP/GCE

advantages favor greater analytical sensitivity, lower LOD, and reduce concomitant interference. This significant improvement of analytical signal indicates the importance of using the hybrid material integrated with carbon nanotubes for the development of a sensitive and robust electroanalytical procedure for AA determination.

Effect of TiO$_2$-Au NPs loading on the modified GCE

The CV was used to investigate the effect of the TiO$_2$-Au NPs hybrid material loading in the analytical response of 0.10 mmol L^{-1} AA in 0.10 mol L^{-1} KCl solution. For this, aliquots of 25 μL, 50 μL or 75 μL of TiO$_2$-Au NPs solution were added in 100 μL of the suspension containing MWCNT/DHP. A higher analytical signal was observed for the electrode which was modified with the solution containing 50 μL of hybrid material (data not shown), and it was chosen

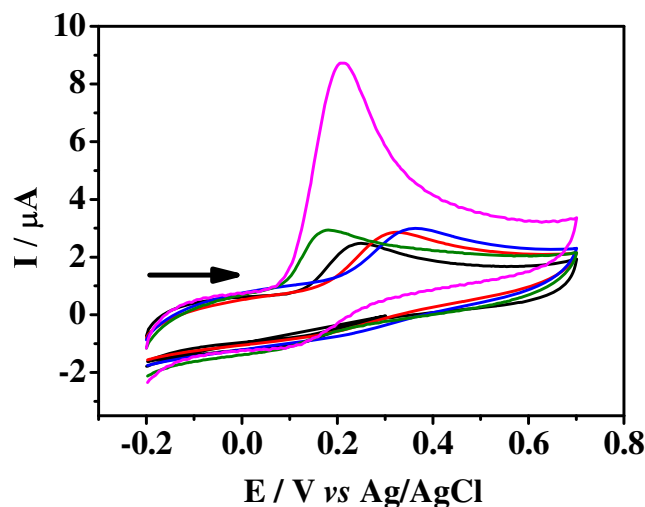for all further electrochemical experiments. The increase of the amount of hybrid material can cause agglomeration in the film formed on GCE, which may reduce the number of active sites, consequently, a decreased of conductive surface of the electrode. In addition, this amount of hybrid material integrated with carbon nanotubes in DHP film provides a homogeneous and adherent film on GCE surface, presenting reproducible responses, without losses of both materials to the solution during the electrochemical measurements. The fabrication reproducibility of the TiO$_2$-Au NP-MWCNT-DHP/GCE was assessed in three different electrodes using the same and three different dispersions for 0.30 mmol L^{-1} AA in 0.10 mol L^{-1} KCl solution. These electrodes and dispersions were obtained independently by the same procedure. Relative standard deviation (RSD) values of 4.73% for the same dispersion and 5.7% for the 3 different dispersions were obtained among these three electrodes, indicating excellent repeatability in the preparation of this modified electrode. The stability of the TiO$_2$-Au NP-MWCNT-DHP/GCE was evaluated by measuring the oxidation current values for 0.10 mmol L^{-1} AA in 0.10 mol L^{-1} KCl solution. Compared to the originally oxidation current value, on the modified electrode there is a decrease of only 5.0% of its original response after 40 measurements, indicating the good stability of the film formed on the GCE surface.

The electrochemical behavior of 0.10 mmol L^{-1} AA at TiO$_2$-Au NP-MWCNT-DHP/GCE was performed in different supporting electrolytes at concentration of 0.10 mol L^{-1}: KCl, KNO$_3$, NaCl and NaNO$_3$. No significant potential displacement in the AA oxidation was observed when these salts were employed (as can be seen in Table S2 (Supplementary materials)), however, the voltammetric response for AA in 0.10 mol L^{-1} KCl solution was characterized by a well-

defined oxidation peak, with higher analytical signal and better repeatability (smaller RSD value). Thus, this supporting electrolyte was selected for the electrochemical determination of AA. The scan rate effect on the peak current was also investigated in order to extract additional electrochemical features of the AA redox process. In Fig. S3a (Supplementary materials), the cyclic voltammograms recorded in the potential scan rate range of 5–400 mV s^{-1} are shown. The peak current increased with a positive shift in the potential when the scan rate increased, a typical characteristic of irreversible electrochemical reaction [31]. A linear plot of the peak current (I_{ap}) vs the scan rate (v) was obtained in the range from 5 to 400 mV s^{-1} in 0.10 mol L^{-1} KCl solution containing 0.10 mmol L^{-1} AA (Fig. S3b (Supplementary materials)), inferring that the redox process at the surface of the working electrode is controlled by the adsorption of the AA on the electrode surface [31]. Considering the negative charges of both electrode surface and the analyte (pK$_a$ 4.17), it was expected a more difficult adsorption process, with a relative lower rate, give rising to an adsorptive controlled electrochemical mechanism. Considering the cyclic voltammogram obtained at 50 mV s^{-1} (Fig. S3a (Supplementary materials)) and applying the following equation $E_{ap} - E_{ap/2} = 0.047/\alpha n$ [32], it was possible estimate the number of electrons transferred (n) in the AA electrooxidation at TiO$_2$-Au NP-MWCNT-DHP/GCE. The AA values of E_{ap} and $E_{ap/2}$ were 0.208 and 0.152 V, respectively. If the value of the transfer coefficient (α) is assumed as equal to 0.5 (which is commonly employed for totally irreversible system), n in the AA electrooxidation was estimated to be equals to two. This results is in agreement with data previously reported in the literature [34], in which AA undergoes oxidation on two hydroxyl groups with the formation of dehydroascorbic acid, as can be observed in Fig. S4 (Supplementary materials).

Evaluation of the analytical performance

The amperometry procedure was performed by evaluating the effect of applied potential, thus ensuring the significant analytical sensitivity and selectivity for the determination of AA on TiO$_2$-Au NP-MWCNT-DHP/GCE. To fulfill this objective, analytical curves were constructed employing different potential values (0.20, 0.30, 0.40 and 0.50 V) and the amperograms were recorded in supporting electrolyte solution containing different AA concentration levels. It was observed that using 0.50 V it was obtained a very high current noise, and this potential was disregarded. The statistical parameters of the constructed analytical curves as sensitivity, adjusted determination coefficient (R^2_a), F value of regression (F_{reg}) and the significance (p), are placed in Table 1. The different analytical curves obtained at 0.2, 0.3, and 0.4 V, showed to be linear with R^2_a close to 1. These results are reinforced because the F_{reg} values are higher than the $F_{critical}$ value ($p \leq 0.001$) [35].

Table 1 Statistical parameters of the analytical curves obtained by amperometry at different potentials

Potential / V	Sensitivity / μA mol^{-1} L	R^2_a	F_{reg}*	p
0.2	2.82×10^3	0.975	156.32	= 0.001
0.3	3.99×10^3	0.995	856.11	< 0.001
0.4	3.59×10^4	0.999	6190.23	< 0.001

* $F_{(1,6)} = 5.99$

Considering that the analytical curves were linear, the best response in terms of sensitivity was obtained using the potential of 0.40 V, thus, this potential value was used. The analytical curve is shown in Fig. 5 and the respective linear regression equation obtained was $I_{ap}/\mu A = -0.059 + 3.59 \times 10^4$ [AA]/mol L^{-1}, which was selected for AA determination in different sample types. The inset in Fig. 5 presents the amperogram of the analytical curve recorded at 0.40 V potential. The calculated LOD value was 1.2 μmol L^{-1}.

The intra-day and inter-day repeatability of the method for the AA determination was evaluated employing TiO$_2$-Au NPs-MWCNTs-DHP/GCE. For intra-day repeatability, 10 successive measurements were performed for a 10 μmol L^{-1} AA solution and the RSD obtained was 4.0%. For inter-day repeatability, 10 μmol L^{-1} AA solutions were used to perform measurements during five consecutive days, maintaining the same conditions. The RSD obtained was 4.2%. This set of results indicates a high precision and repeatability of the measurements obtained using the TiO$_2$-Au NPs-MWCNTs-DHP/GCE and amperometry.

A comparison between the results obtained by using our GCE and amperometry with those reported in the literature for AA determination is presented in Table 2. As can be seen, the GCE combines some advantages
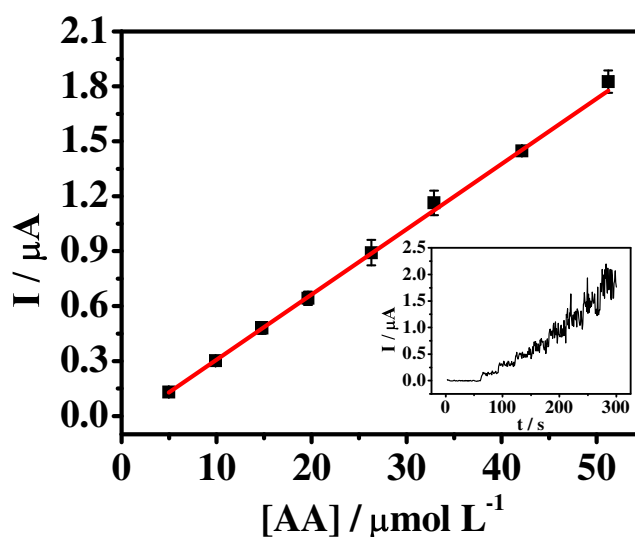

Fig. 5 Calibration plot obtained using the modified GCE in 0.10 mol L^{-1} KCl containing different concentrations of AA: 5.0–51 μmol L^{-1} and amperograms (inset); potential of 0.40 V

Table 2 Comparison of analytical parameters using different electrodes modified with nanostructured materials for the AA determination

Electrode	Technique	Linearity (μmol L^{-1})	LOD (μmol L^{-1})	Reference	Comment
MnFe$_2$O$_4$-MWCNT/GCE	SWV	2.0–100	1.8	[5]	- High LOD. - Argon atmosphere needed.
Au NPs-DMT/Au	Amperometry	0.05–0.40	0.05	[6]	- Expensive equipment and electrodes materials. - Small linear concentration range. - Lower LOD
Au NPs-TiO$_2$/Ti	CV	100–500	–	[7]	- Elaborate fabrication steps. - High linear concentration range. - Hazardous and pollutant materials. - Contamination of analyst
RGO/GCE	DPV	40–1000	4.6	[8]	- Hazardous and pollutant materials. - Multi-step fabrication processes. - Tedious fabrication steps.
Tantegraphene-ANF-C700/GCE	DPV	0.5–60	0.59	[9]	- High temperature. - Pollutant materials. - Tedious fabrication steps. - Requires deoxygenation of the cell.
PtCu alloy/GCE	DPV	25–80	17.5	[10]	- High LOD and small linear concentration range. - Toxic electrode material. - Contamination of analyst.
TiO$_2$-Au NPs-MWCNTs-DHP/GCE	Amperometry	5.0–51	1.2	This work	- Reproducible and stable electrode. - No need pretreatment. - Economic electrode materials. - Simple fabrication process. - Time-consuming preparation of hybrid material - Monodisperse size and uniform dispersion of Au NPs.

Legend: SWV – Square wave voltammetry; DPV – Differential pulse voltammetry.

over previous works [5–10], such as economic fabrication process of the hybrid material although it represents a time-consuming step, guaranteeing an ease control of the size of the Au NPs on TiO$_2$ surface, high stability and reproducibility of sensor besides that the method did not make use of hazardous materials or solvents. Therefore, this electrode can be an alternative to these other modified electrodes for AA determination, showing the feasibility of explore of TiO$_2$-Au NPs hybrid material integrated with carbon nanotubes for the development of a novel amperometric sensor.

Selectivity and other advantages of the modified electrode

The amperometric determination of AA was investigated aiming at assessing the selectivity of the method, the influence of some concomitant compounds typically found in pharmaceutical and food samples. In these experiments, amperometric measurements were performed for a 0.10 mol L^{-1} KCl solution containing 0.10 mmol L^{-1} AA in the presence and absence of each concomitant compound. The chemical compounds tested in these studies were sodium bicarbonate, citric acid, sodium benzoate, magnesium stearate, silicium dioxide and sulfite at concentration ratios of 1:1, 1:10 and 10:1 (analyte:concomitant). Among these compounds, no significant changes were observed in the peak current of AA, indicating that they do not present significant interference (< 3.0%) in the AA determination, as it was confirmed with the addition and recovery study.

UA, DA and sulfite presents distinct oxidation peaks when compared with AA by using CV, revealing other potentialities for application of this novel modified electrode (Fig. S5 (Supplementary materials)).

Application of the analytical method

The amperometric procedure using the TiO$_2$-Au NP-MWCNT-DHP/GCE as an electrochemical sensor was

Table 3 Results obtained from analysis of AA in pharmaceutical and orange juice samples

Sample	Label value	Amperometry[a]	Reference[a]	E (%)[b]
Tablets	500 mg tablet^{-1}	484 ± 3 mg tablet^{-1}	478 ± 4 mg tablet^{-1}	1.3
Orange juice	70 mg mL^{-1}	63.2 ± 1.7 mg mL^{-1}	64.9 ± 1.8 mg mL^{-1}	−2.6

[a] Average of 3 measurements

[b] Relative error (%) = 100 × ([amperometric method – reference method]/reference method)

applied for AA determination in pharmaceutical and orange juice samples. The electrochemical determination was carried out in triplicate ($n = 3$) by amperometry. The results were compared with those provided by a reference procedure (iodometric titration [25]) (Table 3). By comparing the results of this and reference procedures for the two different samples, low RSDs were observed between the results of both the methods. Furthermore, by applying the t-test for difference in means, the value of $t_{\text{calculated}}$ (2.55 and 1.38 for pharmaceutical and fruit juice, respectively) was lower than the critical t value ($t_{\text{critical}} = 2.78$), indicating that this procedure has good accuracy, since there was no significant difference between the results obtained at a confidence level of 95%.

An addition and recovery study was performed by adding known amounts of standard solutions to a given sample followed by analysis using the modified electrode. In both cases, excellent recovery percentages were achieved for the analyzed samples, ranging from 97.7% to 104%, and 96.3 to 105%, respectively, for the pharmaceutical and fruit juice. These results indicate that this method does not suffer from any significant effects of matrix interference.

Conclusion

TiO$_2$-Au NPs hybrids integrated with MWCNTs was used for the modification of GCE. A significant increase of electrochemical signal and a decrease in the overpotential for AA was obtained with respect to the GCE by using the modified electrode. The modified GCE was applied for reliable determination of AA in various sample types of samples using amperometry. Results were similar with those obtained by the iodometric titration method. Moreover, the addition and recovery studies indicated that the matrix effect did not present any significant interference. Intra- and inter-day repeatability studies showed excellent stability of the TiO$_2$-Au NPs hybrid material integrated with carbon nanotubes in DHP film. In addition, this electrode showed potentiality for the simultaneous determination of AA and sulfite and, also of AA with analytes of biological interest (UA and DA). Therefore, the results demonstrated that this modified electrode exhibits very good repeatability and stability under the applied conditions, representing an advanced and effective alternative platform for AA determination.

Compliance with ethical standards The authors declare that they have no competing interests.

References

1. Marsanasco M, Calabró V, Piotrkowski B, Chiaramoni NS, del V. Alonso S (2016) Fortification of chocolate milk with omega-3, omega-6, and vitamins E and C by using liposomes. Eur J Lipid Sci Technol 118:1271–1281. https://doi.org/10.1002/ejlt.201400663

2. Varvara M, Bozzo G, Disanto C, et al (2016) The use of the ascorbic acid as food additive and technical-legal issues. Ital J Food Saf 5.https://doi.org/10.4081/ijfs.2016.4313

3. Radovan C, Cofan C, Cinghita D (2008) Simultaneous determination of acetaminophen and ascorbic acid at an unmodified boron-doped diamond electrode by differential pulse voltammetry in buffered media. Electroanalysis 20:1346–1353. https://doi.org/10.1002/elan.200804188

4. Ngai KS, Tan WT, Zainal Z et al (2013) Voltammetry detection of ascorbic acid at glassy carbon electrode modified by single-walled carbon nanotube/zinc oxide. Int J Electrochem Sci 8:10557–10567

5. Fernandes DM, Silva N, Pereira C, Moura C, Magalhães JMCS, Bachiller-Baeza B, Rodríguez-Ramos I, Guerrero-Ruiz A, Delerue-Matos C, Freire C (2015) MnFe2O4@CNT-N as novel electrochemical nanosensor for determination of caffeine, acetaminophen and ascorbic acid. Sensors Actuators B Chem 218:128–136. https://doi.org/10.1016/j.snb.2015.05.003

6. Kannan P, John SA (2009) Determination of nanomolar uric and ascorbic acids using enlarged gold nanoparticles modified electrode. Anal Biochem 386:65–72. https://doi.org/10.1016/j.ab.2008.11.043

7. Hosseini MG, Faraji M, Momeni MM (2011) Application of titanium oxide nanotube films containing gold nanoparticles for the electroanalytical determination of ascorbic acid. Thin Solid Films 519:3457–3461. https://doi.org/10.1016/j.tsf.2010.12.239

8. Aneesh PK, Nambiar SR, Rao TP, Ajayaghosh A (2014) Electrochemically synthesized partially reduced graphene oxide modified glassy carbon electrode for individual and simultaneous voltammetric determination of ascorbic acid, dopamine and uric

acid. Anal Methods 6:5322–5330. https://doi.org/10.1039/c4ay00043a

9. Taleb M, Ivanov R, Bereznev S, Kazemi SH, Hussainova I (2017) Ultra-sensitive voltammetric simultaneous determination of dopamine, uric acid and ascorbic acid based on a graphene-coated alumina electrode. Microchim Acta 184:4603–4610. https://doi.org/10.1007/s00604-017-2510-y

10. Zhao D, Fan D, Wang J, Xu C (2015) Hierarchical nanoporous platinum-copper alloy for simultaneous electrochemical determination of ascorbic acid, dopamine, and uric acid. Microchim Acta 182:1345–1352. https://doi.org/10.1007/s00604-015-1450-7

11. Parola S, Julián-López B, Carlos LD, Sanchez C (2016) Optical properties of hybrid organic-inorganic materials and their applications. Adv Funct Mater 26:6506–6544. https://doi.org/10.1002/adfm.201602730

12. Eder D (2010) Carbon nanotube−inorganic hybrids. Chem Rev 110:1348–1385. https://doi.org/10.1021/cr800433k

13. Cho ES, Coates NE, Forster JD, Ruminski AM, Russ B, Sahu A, Su NC, Yang F, Urban JJ (2015) Engineering synergy: energy and mass transport in hybrid nanomaterials. Adv Mater 27:5744–5752. https://doi.org/10.1002/adma.201500130

14. Kaur B, Srivastava R (2015) Simultaneous determination of epinephrine, paracetamol, and folic acid using transition metal ion-exchanged polyaniline–zeolite organic–inorganic hybrid materials. Sensors Actuators B Chem 211:476–488. https://doi.org/10.1016/j.snb.2015.01.081

15. Sarhangzadeh K (2015) Application of multi wall carbon nanotube–graphene hybrid for voltammetric determination of naproxen. J Iran Chem Soc 12:2133–2140. https://doi.org/10.1007/s13738-015-0690-0

16. Matthews FL, Rawlings RD (2008) Composite materials: engineering and science. CRC Press

17. Welch CM, Compton RG (2006) The use of nanoparticles in electroanalysis: a review. Anal Bioanal Chem 384:601–619. https://doi.org/10.1007/s00216-005-0230-3

18. Jiang K, Eitan A, Schadler LS, Ajayan PM, Siegel RW, Grobert N, Mayne M, Reyes-Reyes M, Terrones H, Terrones M (2003) Selective attachment of gold nanoparticles to nitrogen-doped carbon nanotubes. Nano 3:275–277. https://doi.org/10.1021/NL025914T

19. Kim B, Sigmund WM (2004) Functionalized multiwall carbon nanotube/gold nanoparticle composites. Langmuir 20:8239–8242. https://doi.org/10.1021/LA049424N

20. Xu C, Chen J, Cui Y, Han Q, Choo H, Liaw PK, Wu D (2006) Influence of the surface treatment on the deposition of platinum nanoparticles on the carbon nanotubes. Adv Eng Mater 8:73–77. https://doi.org/10.1002/adem.200500179

21. Zhou L, Ziong W, Liu S (2015) Preparation of a gold electrode modified with au–TiO2 nanoparticles as an electrochemical sensor for the detection of mercury(II) ions. J Mater Sicence 50:769–776. https://doi.org/10.1007/s10853-014-8636-y

22. Ampelli C, Leonardi SG, Genovese C, Lanzafame P, Perathoner S, Centi G, Neri G (2015) Monitoring of glucose in fermentation processes by using au/TiO2 composites as novel modified electrodes. J Appl Electrochem 45:943–951

23. Damato TC, de Oliveira CCS, Ando RA, Camargo PHC (2013) A facile approach to TiO2 colloidal spheres decorated with au nanoparticles displaying well-defined sizes and uniform dispersion. Langmuir 29:1642–1649. https://doi.org/10.1021/la3045219

24. dos Reis FVE, Antonin VS, Hammer P, Santos MC, Camargo PHC (2015) Carbon-supported TiO2–au hybrids as catalysts for the electrogeneration of hydrogen peroxide: investigating the effect of TiO2 shape. J Catal 326:100–106. https://doi.org/10.1016/j.jcat.2015.04.007

25. British Pharmacopoeia Commission (2013) British pharmacopoeia, 5th ed. The Stationery Office, London

26. Sartori ER, Vicentini FC, Fatibello-Filho O (2011) Indirect determination of sulfite using a polyphenol oxidase biosensor based on a glassy carbon electrode modified with multi-walled carbon nanotubes and gold nanoparticles within a poly(allylamine hydrochloride) film. Talanta 87:235–242. https://doi.org/10.1016/j.talanta.2011.10.003

27. Ardila JA, Oliveira GG, Medeiros RA, Fatibello-Filho O (2013) Determination of gemfibrozil in pharmaceutical and urine samples by square-wave adsorptive stripping voltammetry using a glassy carbon electrode modified with multi-walled carbon nanotubes within a dihexadecyl hydrogen phosphate film. J Electroanal Chem 690:32–37. https://doi.org/10.1016/J.JELECHEM.2012.11.038

28. Al-Otaify A, Leontiadou MA, dos Reis FVE et al (2014) Size dependence of ultrafast charge dynamics in monodisperse au nanoparticles supported on TiO2 colloidal spheres. Phys Chem Chem Phys 16:14189–14194. https://doi.org/10.1039/c4cp01475h

29. Janegitz BC, Baccarin M, Raymundo-Pereira PA, dos Santos FA, Oliveira GG, Machado SAS, Lanza MRV, Fatibello-Filho O, Zucolotto V (2015) The use of dihexadecylphosphate in sensing and biosensing. Sensors Actuators B Chem 220:805–813. https://doi.org/10.1016/j.snb.2015.06.020

30. Suresh S, Gupta M, Kumar GA, Rao VK, Kumar O, Ghosal P (2012) Synergic effect of multi-walled carbon nanotubes and gold nanoparticles towards immunosensing of ricin with carbon nanotube–gold nanoparticles–chitosan modified screen printed electrode. Analyst 137:4086–4092. https://doi.org/10.1039/c2an35279f

31. Gosser DK (1993) Cyclic voltammetry: simulation and analysis of reaction mechanisms. John Wiley & Sons, Inc., New York

32. Bard AJ, Faulkner LR (2001) Electrochemical methods : fundamentals and applications, 2nd edn. John Wiley & Sons, New York

33. Lvovich VF (2012) Impedance spectroscopy: applications to electrochemical and dielectric phenomena. John Wiley & Sons, Inc., Hoboken

34. Yilmaz S, Sadikoglu M, Saglikoglu G et al (2008) Determination of ascorbic acid in tablet dosage forms and some fruit juices by DPV. Int J Electrochem Sci 3:1534–1542

35. Miller JM, Miller JC (2010) Statistics and Chemometrics for analytical chemistry, 6th edn. Pearson, Harlow